

Cite this: *Analyst*, 2015, **140**, 5920

Understanding the cryotolerance of lactic acid bacteria using combined synchrotron infrared and fluorescence microscopies

Stéphanie Passot,^{*a,b} Julie Gautier,^{b,a} Frédéric Jamme,^c Stéphanie Cenard,^{b,a} Paul Dumas^c and Fernanda Fonseca^{b,a}

Freezing is widely used for preserving different types of cells. Frozen concentrates of lactic acid bacteria (LAB) are extensively used for manufacturing food, probiotic products and for green chemistry and medical applications. However, the freezing and thawing processes cause cell injuries that result in significant cell death. Producing homogeneous bacterial populations with high cryotolerance remains a real challenge. Our objective was to investigate the biochemical and physiological changes in a LAB model at the cell scale following fermentation and freezing in order to identify cellular biomarkers of cryotolerance. Infrared spectra of individual bacteria produced by applying different fermentation and freezing conditions were acquired using synchrotron radiation-based Fourier-transform infrared (SR-FTIR) microspectroscopy to achieve sub-cellular spatial resolution. Fluorescent microscopy was concomitantly assessed, thus making possible to simultaneously analyse the biochemistry and physiological state of a single cell for the first time. Principal component analysis was used to evaluate changes in cell composition, with particular focus on lipids, proteins and polysaccharides. SR-FTIR results indicated that before freezing, freeze-resistant cells grown in a rich medium presented a high content of CH₃ groups from lipid chains, of cell proteins in an α -helix secondary structure and of charged polymers such as teichoic and lipoteichoic acids that constitute the Gram-positive bacterial wall. Moreover, SR-FTIR microspectroscopy made it possible to reveal cell heterogeneity within the cluster of resistant cells, which was ascribed to the diversity of potential substrates in the growth medium. Freezing and thawing processes induced losses of membrane integrity and cell viability in more than 90% of the freeze-sensitive bacterial population. These damages leading to cell death were ascribed to biochemical modification of cell membrane phospholipids, in particular a rigidification of the cytoplasmic membrane following freezing. Furthermore the freeze-resistant cells remained viable after freezing and thawing but a modification of protein secondary structure was detected by SR-FTIR analysis. These results highlighted the potential application of bimodal analysis by SR-FTIR and fluorescence microscopy to increase our knowledge about mechanisms related to cell damage.

Received 3rd April 2015,
Accepted 18th July 2015
DOI: 10.1039/c5an00654f

www.rsc.org/analyst

Introduction

Cryopreservation is of paramount importance for maintaining biodiversity and for the long-term storage of cellular and tissue biospecimens (biobanking applications). However, many cells do not survive the various stresses induced by the freeze/thaw process (mechanical, physical and chemical) or exhibit significant loss of function upon thawing. A two-factor

hypothesis of cell freezing injury has been described: (i) a “solution effects” injury due to exposure to increasing solute concentrations during slow freezing; and (ii) intracellular ice formation (IIF) during rapid freezing.^{1–3} No direct evidence of intracellular ice formation in cryopreserved bacteria has been reported. Conversely, it was clearly established that at very high cooling rates, no intracellular ice was formed in lactic acid bacteria (LAB), but injuries were caused by cell plasmolysis that occurred during thawing.⁴

Bacteria survival during freezing is therefore highly dependent on the biophysical event of cell dehydration. Cytoplasmic membrane properties play a fundamental role by governing the water efflux from the cell. Membrane permeability to water is influenced by its fluidity property, which is, in turn,

^aAgroParisTech, UMR 782, Thiverval-Grignon, F-78850, France.

E-mail: stephanie.passot@grignon.inra.fr; Fax: +33 (0)1 30 81 55 97;

Tel: +33 (0)1 30 81 59 40

^bINRA, UMR 782, Thiverval-Grignon, F-78850, France

^cSynchrotron SOLEIL, Gif sur Yvette, F-91192, France

governed by the composition and the structure of the lipid bilayer.⁵ Modulation of the membrane lipid composition by fermentation has a substantial influence on membrane biophysical properties and, consequently, on bacterial cryotolerance.^{6–9} The best resistance to freezing of LAB was mainly associated with the presence of unsaturated and cyclic fatty acid in the membrane.^{6–12}

Recently, we thoroughly investigated the membrane properties of two bacteria populations of *Lactobacillus delbrueckii* ssp. *bulgaricus* CFL1 that exhibited different freezing resistance by determining the membrane fatty acid composition and measuring the lipid phase transition by Fourier Transform Infrared (FT-IR) spectroscopy and membrane fluidity using synchrotron fluorescence polarisation microscopy.^{7,13} The freeze-resistant bacteria population appeared to be characterised by a low lipid membrane phase transition (around 0 °C) that made it possible to maintain high membrane fluidity throughout the freezing process and by a high fluidity homogeneity within the cell membrane at sub-zero temperatures.

Changing the fermentation conditions (pH, temperature, culture medium, application of cold-, heat-, or acid-shock treatment at the end of fermentation) induced cellular modifications other than the modification of the membrane fatty acid composition, especially changes in protein synthesis.^{14–18} By changing the hydrophobic and hydrophilic molecular interactions, freezing may potentially affect not only membrane lipids, but proteins, nucleic acids and wall components as well. Cellular components other than membrane lipids can thus play a crucial role in cell cryotolerance, but have been rarely investigated until now.

Fourier-transform infrared (FTIR) spectroscopy is a powerful analytical tool that has been increasingly used over the last decade to characterise cell metabolism and biochemical composition by providing spectral fingerprints of biological macromolecules such as lipids, proteins, nucleic acids and carbohydrates.^{19,20} In microbiology, FTIR spectroscopy has demonstrated its ability to classify and identify foodborne pathogens.^{21–23} An increasing number of research papers that use this technique have emerged in the last years to assess the molecular changes that occur in food-associated microorganisms in response to stress conditions.^{24,25} Such studies have been carried out on bulk samples, providing spectral data that characterise an average of millions of cells. The use of synchrotron radiation as a high brightness source of infrared photons has allowed investigations at the single-cell level (3–5 µm) and has therefore made it possible to explore the heterogeneity of bacterial populations. The potential of synchrotron radiation-based Fourier-transform infrared (SR-FTIR) microspectroscopy for imaging and spatially resolved biochemical analyses at the single-cell scale has been demonstrated for filamentous fungi, yeast and bacteria.^{26–31} A new challenge would be to correlate the infrared spectra of the individual cell to its physiological state in order to identify molecular biomarkers of cell resistance to environmental stresses. Using reverse engineering, it would then be possible to define adequate fermentation conditions for producing bacteria that exhibits high cryotolerance.

The main objective of this work was to perform a bimodal *in situ* analysis at the single-cell level by combining SR-FTIR microspectroscopy and fluorescence microscopy to concomitantly assess the biochemistry and physiological state (enzymatic activity and membrane integrity) of cells of *Lactobacillus delbrueckii* ssp. *bulgaricus* CFL1 (*Lb* CFL1). *Lb* CFL1 is a lactic acid bacteria, a Gram-positive bacteria widely used as a starter for manufacturing cheese, fermented milk, meat, vegetables, bread and healthcare products. In this work, we aimed at addressing the heterogeneity issue of bacterial cell populations following fermentation and freezing by studying their response to culture media and cryoprotective conditions.

Experimental

Bacteria strain, growth conditions and preparation of cell suspensions

Lactobacillus delbrueckii ssp. *bulgaricus* CFL1 (*Lb* CFL1), a model freeze-sensitive LAB strain, was provided by the Laboratoire de Génie et Microbiologie des Procédés Alimentaires (INRA, Thiverval-Grignon, France). Inocula were stored at –80 °C and were thawed at 42 °C for 5 min before inoculation. Two different culture media were used: Man–Rogosa–Sharpe (MRS) broth (Biokar Diagnostics, Beauvais, France) that induced a freeze-resistant bacterial population, and a mild whey-based medium that induced a freeze-sensitive bacterial population.⁷ The mild whey medium was composed of 60 g L^{–1} of whey powder (Eurosérum, Port-sur-Saône, France) supplemented with 5 g L^{–1} of yeast extract (Organotechnie SAS, La Courneuve, France). Bacterial cultures were carried out at 42 °C, as previously described by Gautier *et al.*⁷ Briefly, a batch preculture was prepared by inoculating 1 mL into 30 mL MRS broth medium in a 50 mL bottle incubated at 42 °C for 12 hours. Ten mL of this preculture were then used to inoculate a 500 mL bottle containing 300 mL of MRS broth or mild whey medium, which was incubated for 12 hours under the same conditions until the stationary growth phase was reached. Bacteria cells were harvested by centrifugation (4 °C, 17 000g, 2 min).

Freezing experiments

The bacterial pellets obtained either from the MRS or the mild whey cultures were re-suspended at 4 °C in the same weight of a sterile protective medium (*i.e.*, 50% wt/wt). The protective medium was composed of either 20% (wt/wt) sucrose or 10% (wt/wt) glycerol in saline solution. The two protected bacterial suspensions were aliquoted in cryotubes (2 mL in 5 mL sterile tubes) and then immersed in liquid nitrogen. The frozen samples were stored at –80 °C. Frozen samples were thawed for 2 min in a 40 °C water bath.

Survival rate of bacterial cells

Cell survival rate was assessed by measuring the cultivability of bacteria before and after freezing. The cultivability was determined using the plate count method (colony-forming units, CFU mL^{–1}).

After serial dilutions in saline water, cells were plated onto solid MRS agar and incubated under anaerobic conditions (GENbox 96124; bioMérieux, Marcy l'Etoile, France) at 42 °C for 48 h before cell counting. Results corresponded to geometrical means of at least three counts. Survival rate (%) was determined from colony counts before freezing and after thawing.

Fluorescent probes and bacteria staining protocols

The physiological state of single bacterial cells was assessed before infrared spectra acquisition by recording fluorescence images. Two fluorescent probes, carboxy fluorescein di-acetate (cFDA) and propidium iodide (PI), were used as previously described by Rault *et al.*³² cFDA is widely used to assess cell viability by detecting the intracellular esterase activity. It is a non-fluorescent precursor that readily diffuses across the cell membrane and yields the positively-charged green fluorescent compound, carboxyfluorescein, upon hydrolysis by non-specific cellular esterase. PI is a nucleic acid dye commonly used to assess cell mortality. It is excluded by cells with intact membranes, but can enter cells with damaged membranes. It binds to DNA to form a red fluorescent DNA-complex.

Before staining, cell suspensions of *Lb.* CFL1 (fresh or frozen/thawed) were diluted in McIlvaine buffer (pH 7.3) up to approximately 10^6 cells per mL. McIlvaine buffer is composed of 0.1 M $C_6H_8O_7$ (citric acid) and 0.2 M Na_2HPO_4 (sodium phosphate). One millilitre of the diluted suspension was supplemented with 10 μ L of PI solution (15 mM in distilled water; Sigma-Aldrich, Lyon, France) and 10 μ L of cFDA solution (0.217 mM in acetone; Invitrogen-Molecular Probes, Eragny-sur-Oise, France) and incubated for 10 min at 40 °C (water bath).

Synchrotron FTIR microscopy of bacterial cells

Synchrotron infrared microscopy was performed at the SMIS beamline at the SOLEIL Synchrotron Facility (Saint-Aubin, France). Spectra were recorded on a Continuum XL microscope (ThermoFisher Scientific, Villebon sur Yvette, France) coupled to a Nicolet 5700 FT-IR spectrometer (ThermoFisher Scientific). The microscope includes a motorised sample stage and a liquid nitrogen-cooled mercury cadmium telluride (MCT-A) detector (50 μ m). It operates in confocal mode with dual

apertures and uses a $\times 32$ infinity-corrected Schwarzschildtype Reflachromat objective (0.65 N.A.) and a matching $\times 32$ condenser with the same numerical aperture. Individual spectra were acquired at 4 cm^{-1} spectral resolution, with 256 co-added scans encompassing the mid-IR region from 4000 to 800 cm^{-1} . Both the spectrometer and microscope were continuously purged with dry air to reduce the spectral contribution of water vapour and CO_2 . The microscope is also equipped with a mercury lamp source, dichroic cubes and emission filters, thus allowing infrared and fluorescent measurements.

Details of the experimental procedure for preparing samples for infrared spectra acquisition can be found elsewhere.^{29,30} The stained bacterial samples (fresh or frozen/thawed) were washed twice in deionised water to remove the staining medium and any trace of the fermentation or protective media (sodium chloride, glycerol and sucrose). A 2 μ L bacterial sample drop was then deposited on the base of an IR transparent zinc-selenide (ZnSe) 4-mm-diameter attenuated total reflectance (ATR) hemispherical internal reflection element (refractive index: $n = 2.4$; ISP Optics Corp., Latvia). The sample drop was dried in a desiccator at room temperature for 30 min. The hemisphere was then deposited under the microscope with its base facing a glass slide. Single bacterial cells were localised with the visible objective (Fig. 1). UV fluorescence emission images of each sample were recorded after excitation using a mercury lamp prior to infrared spectra recording. In addition, a free-sample area was located and recorded (*e.g.*, point marked 'B' in Fig. 1C) as a background infrared signal.

Considering the small size of the bacteria (modelled as a cylinder with projected area between 3 and $5\text{ }\mu\text{m}^2$, *i.e.* close or under to the diffraction limit), FTIR spectroscopic imaging in ATR mode was chosen to improve the spatial resolution compared to transmission mode.^{33,34} Due to the high refractive index of ZnSe (2.4), the area scanned using ATR hemisphere element was approximately $3.3\text{ }\mu\text{m}$ at the sample location when using a double path projected aperture mask of $8 \times 8\text{ }\mu\text{m}^2$. This high spatial resolution was obtained without compromising the quality of the infrared signal thanks to the synchrotron infrared radiation. For each condition tested, analyses were carried out on at least 50 small clusters com-



Fig. 1 Schematic representation of light beam crossing the zinc selenide (ZnSe) ATR hemispherical element (A). Due to the refractive index of ZnSe (2.4), a spatial resolution of $3.3\text{ }\mu\text{m}$ could be obtained using a dual mask aperture of $8 \times 8\text{ }\mu\text{m}^2$. Bright field photomicrograph of *Lb.* CFL1 cells, dried on the ATR hemisphere at 10 \times magnification (B) and 32 \times magnification (C). The size of the white aperture "box" is $3.3 \times 3.3\text{ }\mu\text{m}^2$ and indicates the location where the background was measured. The red crosses correspond to individual bacterial cells where infrared spectra were acquired (C).

posed of one to three individual cells. For each infrared spectrum acquired, it was thus possible to associate it with the physiological state of the cell.

Data treatment and statistical analysis

Spectra were subjected to a quality test, which involves analysing spectra for signal-to-noise ratio, signal intensity and water vapour within the predefined limits for each of the criteria.^{35,36} Pre-processing and data analysis were performed using The Unscrambler software (version 10.1, CAMO Process AS, Oslo, Norway). Three spectral regions were defined according to Naumann²⁰ (Fig. 2):

- S1: the region between 3000 and 2800 cm^{-1} that exhibits the C-H stretching vibrations of $-\text{CH}_3$ and $>\text{CH}_2$ functional groups. This region is therefore generally dominated by the spectral characteristics of fatty acid chains of the various membrane amphiphiles (e.g., phospholipids) and by some amino side-chain vibrations.

- S2: the large spectral region between 1800–900 cm^{-1} that includes the amide region (1800–1500 cm^{-1}), the mixed region

(1500–1200 cm^{-1}) composed of complex vibration bands of proteins, fatty acid and phosphate, and the polysaccharide and nucleic acid region (1200–900 cm^{-1}).

- S3, a part of the S2 region: the region between 1800–1500 cm^{-1} dominated by the conformation-sensitive amide I and amide II bands, which are the most intensive bands in the spectra of nearly all bacterial samples.

Raw spectra in the regions S1 and S2 were first smoothed with a 9- and a 13-point smoothing factor, respectively, and then normalized, and baseline-corrected using the extended multiplicative signal correction (EMSC). This makes it possible to separate and characterise the unwanted physical effects (e.g., differences in sample thickness and light scattering) and the desired chemical information.³⁷ Spectra in the S3 region were pre-processed by calculating the inverted second derivative (Savitsky–Golay, order 3, 13-point smoothing factor), followed by normalisation using the EMSC algorithm.

After pre-processing, the data were analysed by principal component analysis (PCA) to study the unsupervised variation pattern in the data. For the sake of clarity, only relevant score and loading plots are shown in the Results and discussion section.

Results and discussion

Bacterial growth medium induced modifications of the biochemical composition of *Lb* CFL1 cells and of their freezing resistance

Lb CFL1 cells grown either in MRS broth or in mild whey medium were frozen by immersion in liquid nitrogen in the presence of cryoprotectants (glycerol or sucrose). The cell cultivability (in number of CFU per mL) was determined before freezing and after thawing and the percentages of survival determined after thawing were calculated (Table 1). Low survival rates (<10%) were observed for cells grown in mild whey medium, whereas high survival rates were obtained for cells grown in MRS broth, regardless of the cryoprotectant added. Other authors have already reported an improvement in the

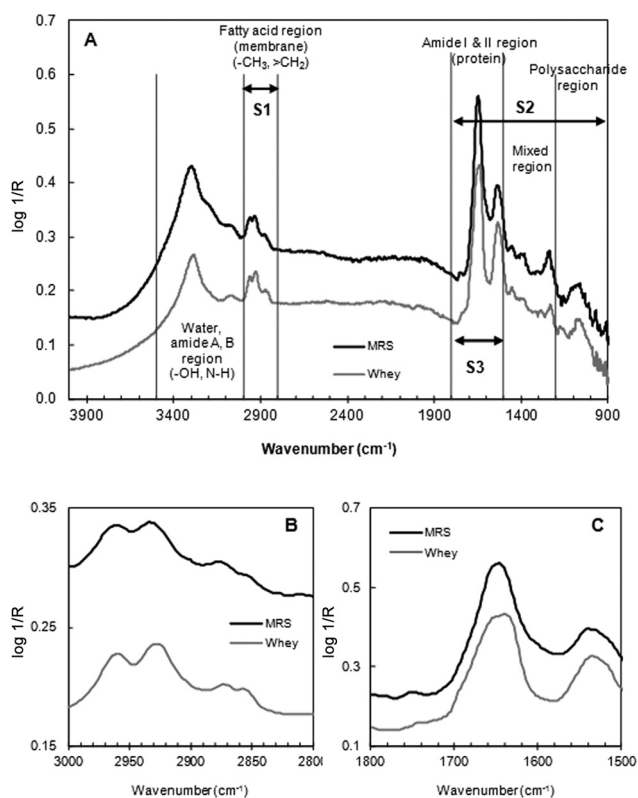


Fig. 2 Representative FTIR raw spectra in the 4000–900 cm^{-1} region of individual cells of the *Lactobacillus delbrueckii* ssp. *bulgaricus* strain CFL1 freshly harvested after growth in MRS broth (black line, MRS) and in mild whey medium (grey line, whey) (A). The spectra are offset in the Y-axis for ease of visualisation. Characteristic molecular group vibrations are indicated as well as the spectral regions (S1, S2 and S3) used for statistical analysis. Enlargement of the lipid (3000–2800 cm^{-1} , S1) and the amide I and II (1800–1500 cm^{-1} , S3) protein regions are displayed in B and C, respectively.

Table 1 Cultivability counts (log CFU mL^{-1}) of *Lactobacillus delbrueckii* ssp. *bulgaricus* CFL1 (*Lb* CFL1) cells determined after fermentation and after freeze–thawing

	Log CFU mL^{-1}		Survival (%)
	After fermentation	After freezing	
MRS – glycerol	10.4 ± 0.6	10.3 ± 0.5	78.2
MRS – sucrose	10.3 ± 0.4	10.2 ± 0.2	81.3
Whey – glycerol	9.8 ± 0.1	8.7 ± 0.1	9.8
Whey – sucrose	9.9 ± 0.7	8.8 ± 0.3	7.2

Survival was determined from colony counts after fermentation and after freezing–thawing and expressed in percentage (%). MRS: *Lb* CFL1 cells were grown in MRS broth. Whey: *Lb* CFL1 cells were grown in mild whey-based medium. Glycerol: *Lb* CFL1 cells were protected by the addition of glycerol before freezing. Sucrose: *Lb* CFL1 cells were protected by the addition of sucrose before freezing.

cryptotolerance of lactic acid bacteria after changing the fermentation conditions (temperature, pH, medium, *etc.*).^{7–9,11,38–41} The improvement of the cell's freezing resistance has previously been linked to the membrane fatty acid composition of lactic acid bacteria, especially to an increase in the cyclopropane fatty acid content^{7,11,12,38} or an increase in the ratio between unsaturated fatty acid and saturated fatty acid.^{6,10} The lipid membrane composition of *Lb* CFL1 grown in MRS broth or in mild whey medium was previously determined by Gautier *et al.*⁷ The membrane of cells grown in MRS broth (inducing freeze-resistant cells) was mainly composed of three fatty acids (FA): C18:1 (48%), C16:0 (18%) and Δ C19:0 (cyclic FA, 14%), whereas the membrane of cells grown in mild whey medium (inducing freeze-sensitive cells) was composed of five fatty acids: C16:0 (38%), C18:1 (22%), C14:0 (9%), C16:1 (7%) and C18:0 (7%).

Furthermore, the modification of culture conditions could also induce the modification of protein synthesis by lactic acid bacteria. When decreasing the temperature of fermentation, lactic acid bacteria synthesized cold shock proteins, which are able to facilitate the translation process under low positive temperatures and to thus protect cells during freezing.^{9,15,42}

Fig. 2A shows the representative raw spectra of individual bacteria grown in MRS broth (black curve) or in mild whey medium (grey curve), illustrating the spectral differences in lipid and protein contents (enlargement Fig. 2B and C). Baseline deformation observed in the 2000–1800 cm^{-1} region arises from a combination of cell morphology and Mie scattering.⁴³ This phenomenon is commonly observed in spectral analysis at sub-cellular level and can induce a change in the amide I band shape and position. No major shift of the amide I band was detected in the recorded bacteria spectra. Assignment of the principal absorption bands was performed using data from the literature on bacteria.²⁰ The spectrum of the “whey cell” is characterised by: (i) more pronounced peaks in the area of the spectrum attributed to the C–H vibration of the CH_2 groups of the membrane fatty acids; and (ii) the shift of the amide I peak towards a lower wavenumber observed for cells grown in mild whey medium (from 1656 cm^{-1} to 1637 cm^{-1}).

Principal component analysis (PCA) was used to identify specific regions of the FTIR spectra that contribute to the discrimination of these two bacterial populations grown using different media. PCA was performed on pre-processed spectra (smoothing and normalisation using EMSC algorithm) of fresh bacteria captured in the lipid region (S1, 3000–2800 cm^{-1}) and the S2 region (between 1800–900 cm^{-1}), involving information about proteins, DNA, RNA and polysaccharides, separately. The first component (PC1) vs. the second component (PC2) score plots and the loading plots of the PC1 for both spectral regions are presented in Fig. 3. Representative fluorescence images of fresh bacterial cells grown either in MRS broth or in whey medium are also displayed (captured with the 10 \times glass objective). Regardless of the growth medium, only green fluorescent cells exhibiting enzymatic activity (*i.e.*, viable cells) were observed. However, when com-

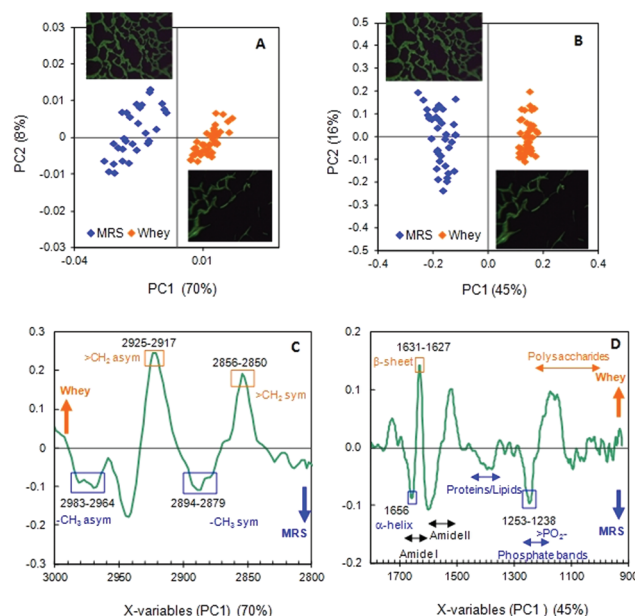


Fig. 3 Principal component analysis (PCA) of infrared spectra obtained after fermentation of bacteria (fresh cells) grown either in MRS broth (MRS, blue symbol) or in mild whey medium (whey, orange symbol). (A) and (B) principal component 1 (PC1) vs. principal component 2 (PC2) score plots in the spectral regions S1 (3000–2800 cm^{-1}) and S2 (1800–900 cm^{-1}), respectively. Insert in (A) and (B): representative fluorescence micrograph of a typical sample of bacteria grown in MRS broth (left) and in mild whey medium (right), like the one from which spectra were taken (10 \times magnification). (C) and (D) corresponding loading plot of the PC1 axis in the spectral regions S1 and S2, respectively. Positive peaks characterised bacterial cells grown in whey medium, whereas negative peaks characterised bacterial cells grown in MRS broth.

paring the spectral data of individual bacteria grown either in MRS broth (MRS cells, blue symbol) or in mild whey medium (whey cells, orange symbol), the PCA score plots showed a clear cluster separation according to the culture medium using the first principal components, regardless of the spectral region considered (S1 or S2). PC2 appeared to be related to cell dispersion within the cluster. Higher cell dispersion (variability) was observed within MRS cells than within whey cells. To assess specific spectral features at the origin of the discrimination between the “MRS cells” and the “Whey cells”, loading plots of PC1 were studied for the S1 and S2 regions (Fig. 3C and D). Major contributions to the spectral variation between MRS and whey cells were the spectral characteristics of fatty acid chains of the amphiphile membranes (phospholipids), amide I and II protein bands, and the phosphate and polysaccharide bands. Positive peaks in the loading plot of the PC1 of the S1 (lipid) and S2 spectral regions correspond to spectral features associated with the bacteria grown in whey medium.

As expected and largely described in the literature, changes in growth medium induced changes in the membrane lipid composition. Bacteria grown in whey medium appeared to be specifically correlated to the C–H stretching vibration of the CH_2 alkyl group (2925–2917; 2856–2850 cm^{-1}) while bacteria

grown in MRS medium were characterised by CH₃ alkyl group (2983–2964; 2894–2879 cm⁻¹). This observation seems well correlated to the lower proportion of cyclic fatty acid and the higher content of saturated fatty acid observed in the membrane of whey cells compared to MRS cells, as reported by Gautier *et al.*⁷

Furthermore, bacteria grown in MRS medium appeared to be specifically correlated to higher contribution of α -helix secondary structure of protein (1656 cm⁻¹) and of charged polymers such as teichoic acids and lipoteichoic acid present in Gram+ bacteria wall (1253–1238 cm⁻¹) than bacteria grown in whey medium which exhibited β -pleated sheet secondary structure (1631–1627 cm⁻¹). The two bacterial populations are thus characterised by different cellular protein contents. Depending on the environmental conditions such as the medium composition bacteria could express differently their genome and synthesise different proteins. To our knowledge, this is the first study reporting such radical differences induced by the modification of the growth medium in terms of the molecular composition of intracellular proteins and cell walls, whereas no difference in the physiological state was detected by fluorescent labelling. These changes could have important consequences on the freezing resistance of bacteria.

When considering the PC2, dispersion within the MRS bacterial population was observed, whereas the fluorescence images revealed a homogeneous viable population (Fig. 3A and B). The loading plots of the PC2 (data not shown) showed that the major contributions to spectral variation within the bacterial population grown in MRS were the symmetric C–H stretching vibration from CH₂ and CH₃ groups, the amide I and the polysaccharide band. Consequently, the dispersion observed within the MRS population could be ascribed to differences in membrane composition, secondary protein structure and cell wall composition among individual cells. MRS broth is a rich culture medium compared to the mild whey-based medium that includes only whey and yeast extract. MRS broth is composed of glucose, peptone, meat and yeast extracts, Tween 80 and salts. Bacteria could thus use a diversity of substrates, allowing cells to differentially express their metabolism.

Works concerning the identification and quantification of bacterial population heterogeneity are scarcely reported in literature. To our knowledge, few studies have investigated the biochemical modification of bacteria during growth using vibrational spectroscopy, in particular Raman microscopy.^{44,45}

Schuster *et al.* studied the feasibility of using Raman spectroscopy to characterize single cell of *C. acetobutylicum* during acetone–butanol fermentation.⁴⁵ In this preliminary study, the number of probed cells (less than 5 per condition) was not enough to enable statistical analysis. Nevertheless, the authors noticed changes in the chemical composition of cells during fermentation, especially changes in polysaccharides, nucleic acids, and proteins content. Choo-Smith *et al.* investigated the spatial heterogeneity of (micro)colonies of *E. coli* and *S. aureus* grown on solid medium over several culture times and at various positions within the colony.⁴⁴ This work is related to

the development of rapid method for the identification of clinically relevant microorganisms using vibrational spectroscopy. Reliable strain identification requires homogeneity within the (micro)colony which seemed possible for young colonies (less than 7 hours of growth). For old (micro)colonies, the Raman spectra measured from various positions and depths within the colony revealed the presence of layers of cells exhibiting different biochemical composition, in particular higher glycogen content for cells located at the surface of the colony. As observed in our study, the polysaccharide band appeared thus to be a marker of bacterial population heterogeneity.

Freezing induced biochemical and physiological changes in *Lb* CFL1 cells

Cell injury induced by freezing has historically been linked to membrane damage. Synchrotron FTIR microspectroscopy made it possible to simultaneously monitor the biochemical and physiological changes of cell components (particularly lipids and proteins) following freezing and thawing, for the first time. The physiological state and infrared spectra of individual cells or small clusters of cells protected with sucrose or glycerol were monitored before and after freeze–thawing. PCA analysis was performed on smoothed spectra in the range of 3000–2800 cm⁻¹ (region S1, lipid region) and on the second derivative in the range of 1800–1500 cm⁻¹ (region S3, amide I and amide II protein region). The PC1 vs. PC2 score plots of the lipid and protein spectral regions computed for all experimental conditions (fresh, frozen/thawed cells, two growth media and two protective media) are presented in Fig. 4 and 5, respectively. Representative fluorescence emission images of stained bacterial cells observed after freezing and thawing are presented in Fig. 4 and 5 for the two growth and protective media used.

Considering bacteria grown in mild whey medium, only red fluorescent cells with damaged membranes and no enzymatic activity were observed for the two cryoprotectants used (sucrose and glycerol). Conversely, green fluorescent cells, *i.e.*, viable cells, were mainly observed for bacteria grown in MRS broth. Few red fluorescent cells (less than 10% of the total cells observed) with damaged membranes were detected after freezing and thawing. No impact of the cryoprotective molecule was observed on the recovery of the physiological state of bacteria after freezing and thawing. These results are in agreement with the survival rates reported in Table 1. Only the infrared spectra from green fluorescent MRS cells obtained after freeze–thawing were included in the multivariate analysis in order to create size-equilibrated groups. In the lipid and protein spectral region (S1 and S3 regions), the PC1 vs. PC2 score plots displayed in Fig. 4 and 5 indicated an unambiguous sample clustering when considering the PC1 due to the nature of the growth medium. As expected, the loading plot of the PC1 (data not shown) revealed the same spectral features as those revealed in Fig. 3. The biochemical modifications induced by the freezing treatment are expected to be less

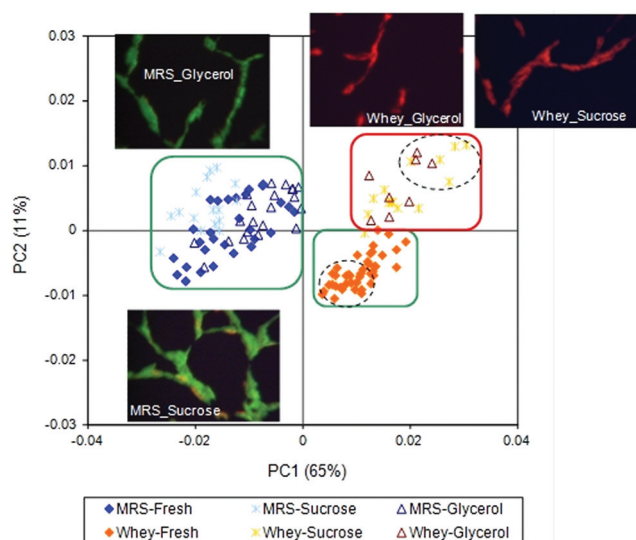


Fig. 4 Principal component analysis (PCA) of infrared spectra obtained after fermentation and after freezing and thawing of bacteria grown either in MRS broth (MRS, blue symbol) or in mild whey medium (whey, orange symbol) and protected by the addition of sucrose or glycerol. The spectral range used for this analysis is the lipid region (S1 region, 3000–2800 cm^{-1}). Insert: representative fluorescence micrograph of a typical sample of bacteria grown in MRS broth (left) and in mild whey medium (right) and frozen in sucrose or glycerol protective solution (32 \times magnification). The second derivative of the average infrared spectra of bacterial cells included in the dotted circles were plotted in Fig. 6.

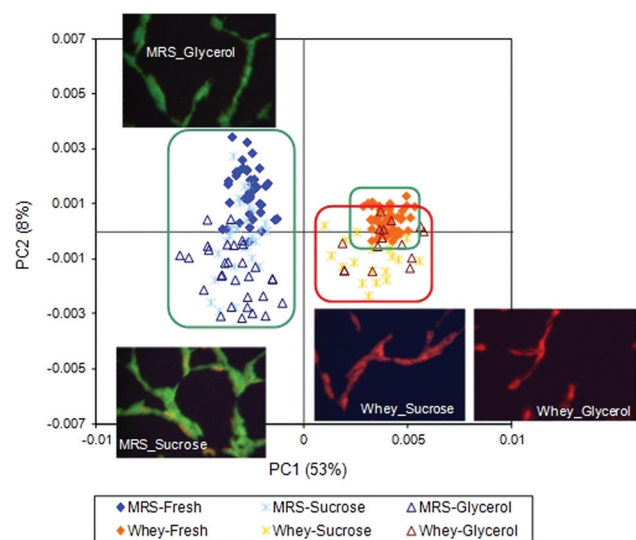


Fig. 5 Principal component analysis (PCA) of second derivative infrared spectra obtained after fermentation and after freezing and thawing of bacteria grown either in MRS broth (MRS, blue symbol) or in mild whey medium (whey, orange symbol) and protected by the addition of sucrose or glycerol. The spectral range used for this analysis is the amide I and II protein region (S3 region, 1800–1500 cm^{-1}). Insert: representative fluorescence micrograph of a typical sample of bacteria grown in MRS broth (left) and in mild whey medium (right) and frozen in sucrose or glycerol protective solution (32 \times magnification).

significant than the biochemical modifications induced by the change in the growth medium.

Biochemical modifications caused by freezing can be clearly identified when considering PC2. The PCA score plot computed in the lipid region (3000–2800 cm^{-1} ; Fig. 4) revealed a clear separation between the fresh and the frozen samples of bacteria grown in mild whey medium, whereas no cluster was observed for bacteria grown in MRS broth. This sample clustering is correlated with the physiological state of bacteria. Bacteria exhibiting membrane damage (“red cells”) are clearly separated from intact bacteria (“green cells”). The major contribution to spectral variation between unfrozen and frozen cells grown in whey medium arose from the C–H stretching vibrations from CH_2 and CH_3 groups (PC2 loading plot not shown). The main cell damage induced by freezing reported in the literature is the loss of membrane integrity.^{7,46–48} The band position of the symmetric C–H stretching vibration of the CH_2 groups is often reported as an indicator of membrane fluidity.⁴⁹ A shift toward a lower wavenumber is associated with membrane rigidification (decrease of membrane fluidity). The second derivatives of the average spectra of two opposite clusters of “whey cells” along the PC2 axis (circles in Fig. 4) were plotted in Fig. 6. Freezing resulted in a shift of the symmetric C–H vibration of the CH_2 groups to a lower wavenumber (from 2854 cm^{-1} to 2850 cm^{-1}) following freezing. Considering the width of the band corresponding to the symmetric C–H vibration of the CH_2 alkyl group (larger than 8 cm^{-1}), this shift of 4 cm^{-1} can be considered as significant even if a spectral resolution of 4 cm^{-1} was applied for spectra acquisition (*i.e.* corresponding to a frequency of data acquisition every 2 cm^{-1}). These changes in the CH_2 groups could be ascribed to a modification in the organisation of the aliphatic chains of membrane lipids following freezing, which in

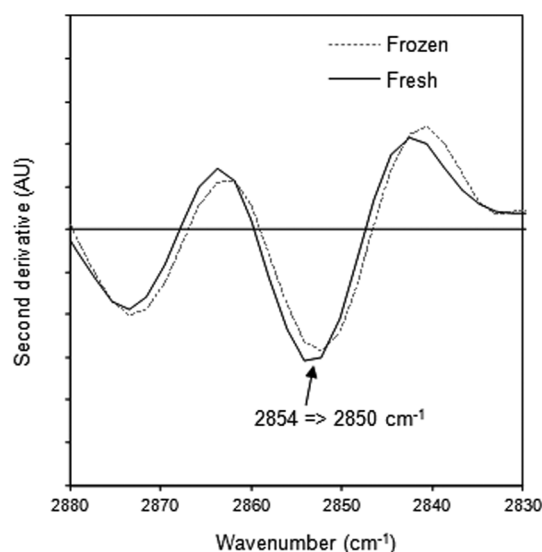


Fig. 6 Second derivative of the mean infrared spectra of fresh and frozen bacterial samples grown in mild whey medium (dotted circles in Fig. 4) in the lipid spectral range (3000–2800 cm^{-1}).

turn could be associated with a rigidification of the membrane and a loss of membrane integrity observed only for cells grown in whey medium. Saulou *et al.* also reported a wavenumber downshift of the symmetric CH_2 stretching peak associated with cell death when *E. coli* cells were exposed to silver ions.²⁹ However, the lipid region ($3000\text{--}2800\text{ cm}^{-1}$) appears to be barely targeted in the analysis by FTIR spectroscopy of the biochemical changes in cells exposed to environmental stresses, compared to the protein region ($1800\text{--}1500\text{ cm}^{-1}$).

Focusing on the amide I and II protein region (Fig. 5), no clear bacteria clustering was observed according to the freezing treatment. However, within the “green cells” grown in MRS broth, the frozen cells protected by glycerol (open blue triangle) appeared to be slightly different from the fresh cells (blue diamond). The frozen cells protected by sucrose (blue cross) overlapped both fresh and frozen cells protected with glycerol. Half of the sucrose samples were indeed close to the unfrozen MRS samples and the other part to the glycerol-frozen samples. The second derivative of the average spectra of the fresh MRS cells and the frozen MRS cells protected with glycerol were plotted in Fig. 7. Following freezing, a wavenumber downshift of the amide I peak from 1658 cm^{-1} to 1637 cm^{-1} was observed, indicating a reduction in α -helical protein content and an increasing content of β -sheet protein. Consequently, freezing resulted in protein conformational changes. Moreover, sucrose appeared to be more efficient to preserve the secondary structure of the protein than glycerol during freezing. In contrast with damages observed on membrane organisation, the protein damages detected on infrared spectra following freezing were not associated with a change in the physiological state of the cell. The protein conformational changes observed in our study did not seem to be detrimental for bacteria viability recovery. Other authors reported protein conformational changes when bacteria are exposed to environmental stresses.^{25,29} Lu *et al.* also reported changes in spectral features in the $1200\text{--}900\text{ cm}^{-1}$ region following freezing of

Gram-negative bacteria, ascribed to the production of oligosaccharides and potentially other components in response to cold stress.²⁵ The infrared spectra of the frozen bacterial samples unfortunately appeared to be too noisy in the $1200\text{--}900\text{ cm}^{-1}$ region to be correctly targeted by multivariate analysis. The small aperture used in this signal ($8 \times 8\text{ }\mu\text{m}$) to reach single-cell spatial resolution strongly increases the noise at the longer wavelengths (wavenumber lower than 1000 cm^{-1}).

Conclusion

In conclusion, this study reported bimodal single-cell analysis by synchrotron FTIR and fluorescence microscopy of bacteria following fermentation and freezing for the first time. By simultaneously acquiring information on the biochemical and physiological properties of cells, we were able to assess relevant spectral biomarkers of the cryotolerance of lactic acid bacteria. Furthermore, the cell heterogeneity in biochemical responses to the fermentation and freezing conditions within the bacterial population was highlighted. Further experiments focusing on other fluorescent probes could potentially allow a more subtle physiological characterisation of cells, which would help to identify the properties of freeze-resistant cells that, in turn, would make it possible to both screen and produce homogenous resistant populations by modifying the fermentation conditions.

Acknowledgements

The research performed in this paper was performed at the French national synchrotron facility SOLEIL (Gif sur Yvette, France), using the SMIS beamline (proposal no 20100789).

References

- 1 P. Mazur, *Cryobiology*, 1977, **14**, 251–272.
- 2 P. Mazur, *Am. J. Physiol.*, 1984, **247**, C125–C142.
- 3 P. Mazur, S. P. Leibo and E. H. Y. Chu, *Exp. Cell Res.*, 1972, **71**, 345–355.
- 4 F. Fonseca, M. Marin and G. J. Morris, *Appl. Environ. Microbiol.*, 2006, **72**, 6474–6482.
- 5 C. D. Stubbs, *Essays Biochem.*, 1983, **19**, 1–39.
- 6 C. Beal, F. Fonseca and G. Corrieu, *J. Dairy Sci.*, 2001, **84**, 2347–2356.
- 7 J. Gautier, S. Passot, C. Penicaud, H. Guillemin, S. Cenard, P. Lieben and F. Fonseca, *J. Dairy Sci.*, 2013, **96**, 5591–5602.
- 8 F. Streit, G. Corrieu and C. Beal, *J. Biotechnol.*, 2007, **128**, 659–667.
- 9 Y. Wang, G. Corrieu and C. Beal, *J. Dairy Sci.*, 2005, **88**, 21–29.
- 10 I. Goldberg and L. Eschar, *Appl. Environ. Microbiol.*, 1977, **33**, 489–496.
- 11 R. B. Smittle, S. E. Gilliland, M. L. Speck and W. M. Walter Jr., *Appl. Microbiol.*, 1974, **27**, 738–743.

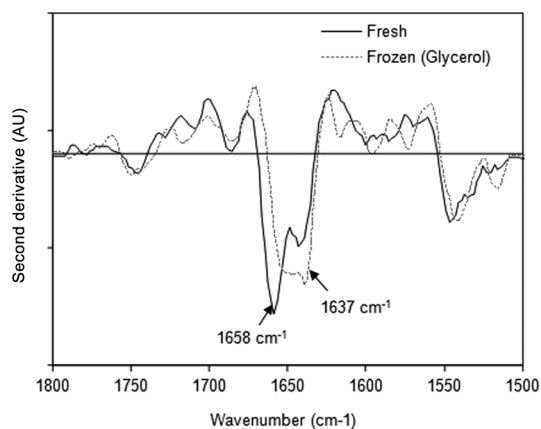


Fig. 7 Second derivative of the mean infrared spectra of fresh and frozen bacterial samples grown in MRS broth and protected by the addition of glycerol in the amide I and amide II protein region ($1800\text{--}1500\text{ cm}^{-1}$).

- 12 A. G. Zavaglia, E. A. Disalvo and G. L. De Antoni, *J. Dairy Res.*, 2000, **67**, 241–247.
- 13 S. Passot, F. Jamme, M. Réfrégiers, J. Gautier, S. Cenard and F. Fonseca, *Biomed. Spectrosc. Imaging*, 2014, **3**, 203–210.
- 14 L. Baati, C. Fabre-Gea, D. Auriol and P. J. Blanc, *Int. J. Food Microbiol.*, 2000, **59**, 241–247.
- 15 W. S. Kim and N. W. Dunn, *Curr. Microbiol.*, 1997, **35**, 59–63.
- 16 G. L. Lorca and G. F. de Valdez, *Cryobiology*, 1999, **39**, 144–149.
- 17 F. Streit, J. Delettre, G. Corrieu and C. Beal, *J. Appl. Microbiol.*, 2008, **105**, 1071–1080.
- 18 Y. Wang, J. Delettre, G. Corrieu and C. Beal, *Biotechnol. Prog.*, 2011, **27**, 342–350.
- 19 Z. Movasaghi, S. Rehman and I. U. Rehman, *Appl. Spectrosc. Rev.*, 2008, **43**, 134–179.
- 20 D. Naumann, in *Encyclopedia of Analytical Chemistry*, ed. R. A. Meyer, John Wiley & Sons Ltd, Chichester, 2000, pp. 102–131.
- 21 H. AlRabiah, E. Correa, M. Upton and R. Goodacre, *Analyst*, 2013, **138**, 1363–1369.
- 22 T. Udelhoven, D. Naumann and J. Schmitt, *Appl. Spectrosc.*, 2000, **54**, 1471–1479.
- 23 C. L. Winder and R. Goodacre, *Analyst*, 2004, **129**, 1118–1122.
- 24 A. Alvarez-Ordóñez, D. J. Mouwen, M. López and M. Prieto, *J. Microbiol. Methods*, 2011, **84**, 369–378.
- 25 X. Lu, Q. Liu, D. Wu, H. M. Al-Qadiri, N. I. Al-Alami, D. H. Kang, J. H. Shin, J. Tang, J. M. Jabal, E. D. Aston and B. A. Rasco, *Food Microbiol.*, 2011, **28**, 537–546.
- 26 L. G. Benning, V. R. Phoenix, N. Yee and M. J. Tobin, *Geochim. Cosmochim. Acta*, 2004, **68**, 729–741.
- 27 F. Jamme, J. D. Vindigni, V. Méchin, T. Chérifi, T. Chardot and M. Froissard, *PLoS One*, 2013, **8**, e74421.
- 28 K. Jilkine, K. M. Gough, R. Julian and S. G. Kaminskyj, *J. Inorg. Biochem.*, 2008, **102**, 540–546.
- 29 C. Saulou, F. Jamme, L. Girbal, C. Maranges, I. Fourquaux, M. Cocaigh-Bousquet, P. Dumas and M. Mercier-Bonin, *Anal. Bioanal. Chem.*, 2013, **405**, 2685–2697.
- 30 C. Saulou, F. Jamme, C. Maranges, I. Fourquaux, B. Despax, P. Raynaud, P. Dumas and M. Mercier-Bonin, *Anal. Bioanal. Chem.*, 2010, **396**, 1441–1450.
- 31 A. Szeghalmi, S. Kaminskyj and K. M. Gough, *Anal. Bioanal. Chem.*, 2007, **387**, 1779–1789.
- 32 A. Rault, C. Beal, S. Ghorbal, J. Ogier and M. Bouix, *Cryobiology*, 2007, **55**, 35–42.
- 33 S. G. Kazarian and K. L. A. Chan, *Analyst*, 2013, **138**, 1940–1951.
- 34 L. L. Lewis and A. J. Sommer, *Appl. Spectrosc.*, 2000, **54**, 324–330.
- 35 D. Helm, H. Labischinski, G. Schallehn and D. Naumann, *J. Gen. Microbiol.*, 1991, **137**, 69–79.
- 36 A. Kohler, D. Bertrand, H. Martens, K. Hannesson, C. Kirschner and R. Ofstad, *Anal. Bioanal. Chem.*, 2007, **389**, 1143–1153.
- 37 A. Kohler, C. Kirschner, A. Oust and H. Martens, *Appl. Spectrosc.*, 2005, **59**, 707–716.
- 38 J. R. Broadbent and C. Lin, *Cryobiology*, 1999, **39**, 88–102.
- 39 F. Fonseca, C. Beal and G. Corrieu, *Cryobiology*, 2001, **43**, 189–198.
- 40 A. Rault, M. Bouix and C. Béal, *Appl. Environ. Microbiol.*, 2009, **75**, 4374–4381.
- 41 A. Rault, M. Bouix and C. Béal, *Int. Dairy J.*, 2010, **20**, 792–799.
- 42 P. Graumann, T. M. Wendrich, M. H. W. Weber, K. Schroder and M. A. Marahiel, *Mol. Microbiol.*, 1997, **25**, 741–756.
- 43 A. V. Rutter, M. R. Siddique, J. Filik, C. Sandt, P. Dumas, G. Cinque, G. D. Sockalingum, Y. Yang and J. Sule-Suso, *Cytometry, Part A*, 2014, **85A**, 688–697.
- 44 L. P. Choo-Smith, K. Maquelin, T. van Vreeswijk, H. A. Bruining, G. J. Puppels, N. A. G. Thi, C. Kirschner, D. Naumann, D. Ami, A. M. Villa, F. Orsini, S. M. Doglia, H. Lamfarraj, G. D. Sockalingum, M. Manfait, P. Allouch and H. P. Endtz, *Appl. Environ. Microbiol.*, 2001, **67**, 1461–1469.
- 45 K. C. Schuster, E. Urlaub and J. R. Gapes, *J. Microbiol. Methods*, 2000, **42**, 29–38.
- 46 L. Cao-Hoang, F. Dumont, P. A. Marechal and P. Gervais, *Arch. Microbiol.*, 2010, **192**, 299–305.
- 47 W. V. Holt, M. F. Head and R. D. North, *Biol. Reprod.*, 1992, **46**, 1086–1094.
- 48 M. Moussa, F. Dumont, J. M. Perrier-Cornet and P. Gervais, *Biotechnol. Bioeng.*, 2008, **101**, 1245–1255.
- 49 A. Alvarez-Ordóñez, J. Halisch and M. Prieto, *Int. J. Food Microbiol.*, 2010, **142**, 97–105.